ORIGINAL ARTICLE

Diallyl sulfide protects against ultraviolet B-induced skin cancers in SKH-1 hairless mouse: analysis of early molecular events in carcinogenesis

Jaw-Ming Cherng[1], Kuen-Daw Tsai[2,3], Daw-Shyong Perng[4], Jeng-Shing Wang[5,6], Cheng-Chung Wei[1] & Jung-Chung Lin[7]

[1]Department of Internal Medicine, Chung Shan Medical University Hospital, Chung Shan Medical University, Taichung, Taiwan, ROC, [2]Department of Internal Medicine, China Medical University and Beigang Hospital, Yunlin, Taiwan, ROC, [3]Institute of Molecular Biology, National Chung Cheng University, Chiayi, Taiwan, ROC, [4]Department of Internal Medicine, E-Da Hospital, I-Shou University, Kaohsiung, Taiwan, ROC, [5]Department of Internal Medicine, Antai Tian-Sheng Memorial Hospital, Pingtung, Taiwan, ROC, [6]Department of Internal Medicine, Taipei Medical University, Taipei, Taiwan, ROC, and [7]Cellular Virology Unit, Centers for Disease Control and Prevention, Division of Viral Hepatitis, Atlanta, GA, USA

Key words:
chemoprevention; diallyl sulfide; skin tumors; ultraviolet

Correspondence:
Jung-Chung Lin, Cellular Virology Unit, Centers for Disease Control and Prevention, Division of Viral Hepatitis, Atlanta, GA 30333, USA.
e-mail: linderson1939@gmail.com

Accepted for publication:
9 February 2011

Conflicts of interest:
None declared.

Summary

Background: Diallyl sulfide (DAS) has been shown to have a preventive effect against various cancers.

Aims and objectives: We evaluated the protective effects of DAS in regression of ultraviolet B (UVB)-induced skin tumor formation in SKH-1 hairless mice and its underlying early molecular biomarkers.

Methods: We examined the efficacy of DAS in UVB light-induced skin lesion in SKH-1 hairless mice and the associated molecular events.

Results: Mice irradiated with UVB at 180 mJ/cm^2 twice per week elicited 100% tumor incidence at 20 weeks. The topical application of DAS before UVB irradiation caused a delay in tumor appearance, multiplicity, and size. The topical application of DAS before and immediately after a single UVB irradiation (180 mJ/cm^2) resulted in a significant decrease in UVB-induced thymine dimer-positive cells, expression of proliferative cell nuclear antigen (PCNA), terminal deoxynucleotidyl transferase-mediated dUTP nick end labeling, and apoptotic sunburn cells, together with an increase in p53 and p21/Cip1-positive cell population in the epidermis. Simultaneously, DAS also significantly inhibited nuclear factor-κB (NF-κB), cyclooxygenase-2 (COX-2), prostaglandin E2 (PGE2), and nitric oxide (NO) levels.

Conclusions: The protective effect of DAS against photocarcinogenesis is accompanied by the down-regulation of cell-proliferative controls, involving thymine dimer, PCNA, apoptosis, transcription factors NF-κB, and of inflammatory responses involving COX-2, PGE2, and NO, and up-regulation of p53, p21/Cip1 to prevent DNA damage and facilitate DNA repair.

Ultraviolet (UV) light has been well documented as a complete carcinogen responsible for the initiation and promotion of both basal and squamous cell carcinomas (1). Direct absorption of UV by DNA leads to the formation of thymine dimers of DNA bases (2). Like many chemical tumor promoters, UV also elicits inflammation, epidermal hyperplasia, and changes in the expression of numerous genes associated with proliferation and differentiation, eicosanoid and cytokine production, and growth factor synthesis and responsiveness (3). This diversity of responses suggests that there are probably multiple processes that could be effective targets for prevention.

Garlic (*Allium sativum* Linn.) has been widely used as a flavoring agent and as a traditional medicine to treat a variety of diseases in many countries, notably the Near East, China, and India (4). Garlic has been documented to exhibit a wide spectrum of pharmacological effects including antioxidant with a radical scavenging effect, a suppressive effect on lipoxygenase and cyclooxygenase activities, anti-inflammatory activity, cellular immunity enhancement, DNA-binding and synthesis inhibition, DNA repair induction, antiproliferative effect, chemopreventive, antimutagenic, and anticarcinogenic effects, and antiviral and antibacteria activities (5). Garlic has already entered various clinical trials (6). Dially sulfide (DAS) is one of the principal components and is found exclusively in garlic (7). DAS and/or other organosulfur compounds of garlic have been found to have antioxidant, anti-inflammatory, and antitumor activities in a variety of animal models of human diseases (5). The mechanisms by which these compounds affect multiple biochemical and inflammatory conditions appear to be cell- and stimulus-specific and to involve effects on the cell's transcriptional machinery such as

nuclear factor-κB (NF-κB), cyclooxygenase-2 (COX-2), and redox homeostasis (8–10). Several clinical studies indicated that DAS exerted an anti-inflammatory activity due in part to the inhibition of inducible isoforms of nitric oxide synthase (iNOS) and COX-2 enzymes (8–10). Nitric oxide (NO) has been proposed to be an important mediator of tumor growth (11) and overexpressed iNOS has also been detected in several human tumors (12). In particular, the inhibition of COX-2 was significant in colon cancer cells, which makes garlic important as a colon cancer preventive agent (13). The inhibition of the COX-2 enzyme is achieved by suppressing the activation of NF-κB, a eukaryotic transcription factor (13).

We assessed the protective effects of DAS against photocarcinogenesis in the SKH-1 hairless mouse skin model (14–16). We found that DAS is a potent inhibitor against UVB-induced skin tumors. We further analyzed the effect of DAS on early biomarkers (17–19) associated with photocarcinogenesis. Our results suggest that DAS has a protective effect against UVB-caused damage in the epidermis by decreasing thymine dimer formation, increasing p53–p21/Cip1 expression, and inhibiting both NF-κB and COX-2, leading to suppressions of NO and prostaglandin E2 (PGE2), and cell proliferation and apoptosis.

Table 1. Experimental design depicting the variables and treatment groups both in the long-term and in the short-term study

Exposure	No DAS	DAS first	DAS last
No UVR	a (Control)	b (DAS-T)	–
UVR	c (UV)	d (DAS-T+UV)	e (UV+DAS-T)

Mice were divided into five groups: a, b, c, d, and e. Twenty mice per group were included for the long-term study and five mice per group for the short-term study.
UVR, UVB irradiation (180 mJ/cm^2), twice/week for the long-term study and single exposure for the short-term study.
DAS-T, topical application of DAS, twice/week for 26 weeks (long-term study) and once for the short-term study.
DAS-T+UV, topical application of DAS 30 min before UVB; UV+DAS-T, topical application of DAS immediately after UVB irradiation.
DAS, diallyl sulfide; UV, ultraviolet.

Materials and methods

Animals, UV light source and chemical

Inbred female SKH-1 hairless mice (5 weeks old) were purchased from Charles River Laboratories (Wilmington, MA, USA) and maintained in accordance with relevant guidelines and regulations for the care and use of laboratory animals of China Medical University.

The UVB light source consisted of four FS40T12/UVB sunlamps (Philips, Amsterdam, the Netherlands), which emitted ∼80% radiation in the range of 280–340 nm with a peak emission at 314 nm as monitored using an SED240 photodetector with an SPS300 filter, and a T input optic connected to an ILT1700 Research Radiometer (International Light Technologies, Newburyport, MA, USA). The SPS300 filter removes wavelengths shorter than 280 nm and with the predominant emitting peak at 280–315 nm. The radiometer is calibrated on a regular basis against both a traceable standard lamp and the laboratory radiation source.

Mice were exposed to UVB irradiation for 2 min and 40 s with a distance of 23 cm between the light source and the target skin.

DAS was purchased from Sigma-Aldrich, Inc. (St Louis, MO, USA) and was solubilized in acetone.

Experimental designs

Both long- and short-term studies were conducted to assess the effect of DAS on UVB-induced skin photocarcinogenesis in female SKH-1 hairless mice. The experimental design, variables, and treatment groups are depicted in Table 1. The long-term regimen was designed to assess the effect of DAS on UVB-induced skin tumor incidence, whereas the short-term study was for assessing early molecular biomarkers. 1-h samples were used for the analysis of thymine dimer formation; 8-h samples for p53, p21/Cip1, proliferative cell nuclear antigen (PCNA), NF-κB, COX-2, PGE2, and NO; and 12-h samples for the TUNEL assay and apoptotic sunburn cells.

Immunohistochemical analysis of biomarkers

The apoptotic cells were detected using the Dead End Colorimetric TUNEL system (Promega Corporation, Madison, WI, USA) according to the manufacturer's instructions. The apoptotic sunburn cells were stained conventionally with H&E and examined using light microscopy.

To detect thymine dimer-positive cells, the antithymine dimer antibody (Kamiya Biomedical Company, Seattle, WA, USA) was used. Activities were then detected using the NovoLink Polymer Detection System (Novocastra Laboratories, Newcastle Upon Tyne, UK).

For the detection of p53, p21/Cip1, and PCNA, mouse monoclonal anti-p53 (LifeSpan BioSciences, Seattle, WA, USA), anti-p21/Cip1 (Acris Antibodies GmbH, Herford, Germany), or anti-PCNA (Biocare Medical, Concord, CA, USA) antibodies were used. Activities were detected using the NovoLink Polymer Detection System (Novocastra Laboratories).

The microscopic examinations were performed by two investigators in a blinded fashion. For every specimen, five to 10 randomly selected fields were examined and counted at × 400 magnification. Data were calculated as mean ± standard error (SE) of 25 fields/5 mice/group.

Biochemical analysis of NO, COX-2, and PGE2 activities

The frozen skin specimens were pulverized in liquid nitrogen. The powder was suspended in cell lysis buffer (20) and sonicated before centrifugation at 12 500 × g for 20 min. The supernatants were collected and used for the quantitative analysis of NO

(BioVision, Mountain View, CA, USA), COX-2 (USCN LIFE (Wuhan, China), and PGE2 (R&D System, Minneapolis, MN, USA), using ELISA kits following the manufacturer's protocols.

Analysis of NF-κB DNA-binding activity

For analyzing transcription factor NF-κB-binding activity to DNA, nuclear proteins were prepared as described previously (20) and the binding activity was quantified using the TF ELISA kit (Panomics, Fremont, CA, USA) following the manufacturer's protocol. This method is faster, easier, and more sensitive than electrophoretic mobility shift assays and does not require the use of radioactivity.

Statistical analysis

Data were presented as means ± SE. The evaluation of statistical significance was determined by one-way analysis of variance (ANOVA), followed by the Bonferroni t-test for multiple comparisons. A P value < 0.05 was considered statistically significant.

Results

Protective effects of DAS on UVB-induced tumorigenesis in SKH-1 hairless mouse

Figure 1 shows that the topical application of DAS delayed the appearance of the first tumor. The first tumor appearance in UVB-alone animals occurred in the 16th week, which was delayed by 3 weeks in the DAS-pretreated group (DAS-T+UV) and by 2 weeks in the post-treated group (UV+DAS-T). UVB irradiation at 180 mJ/cm^2 twice per week caused 100% tumor incidence after 20 weeks in the UVB-alone group, 23 weeks in the post-treated group, and 24 weeks in the pretreated group (Fig. 1a). Compared with the UVB-alone group (Fig. 1b), both pre- and post-DAS treatment reduced the number of tumors per mouse throughout the experiment and showed 49% and 38% decrease ($P < 0.001$), respectively, in tumor multiplicity. Tumor volume per tumor per mouse (Fig. 1c) was also decreased from 388 ± 44 mm^3 in the UVB-alone group to 136 ± 13 and 164 ± 17 mm^3 in the DAS pre-treated and post-treated groups, respectively, accounting for 65% and 58% decrease ($P < 0.005$). No tumors were observed in the control and DAS-alone groups

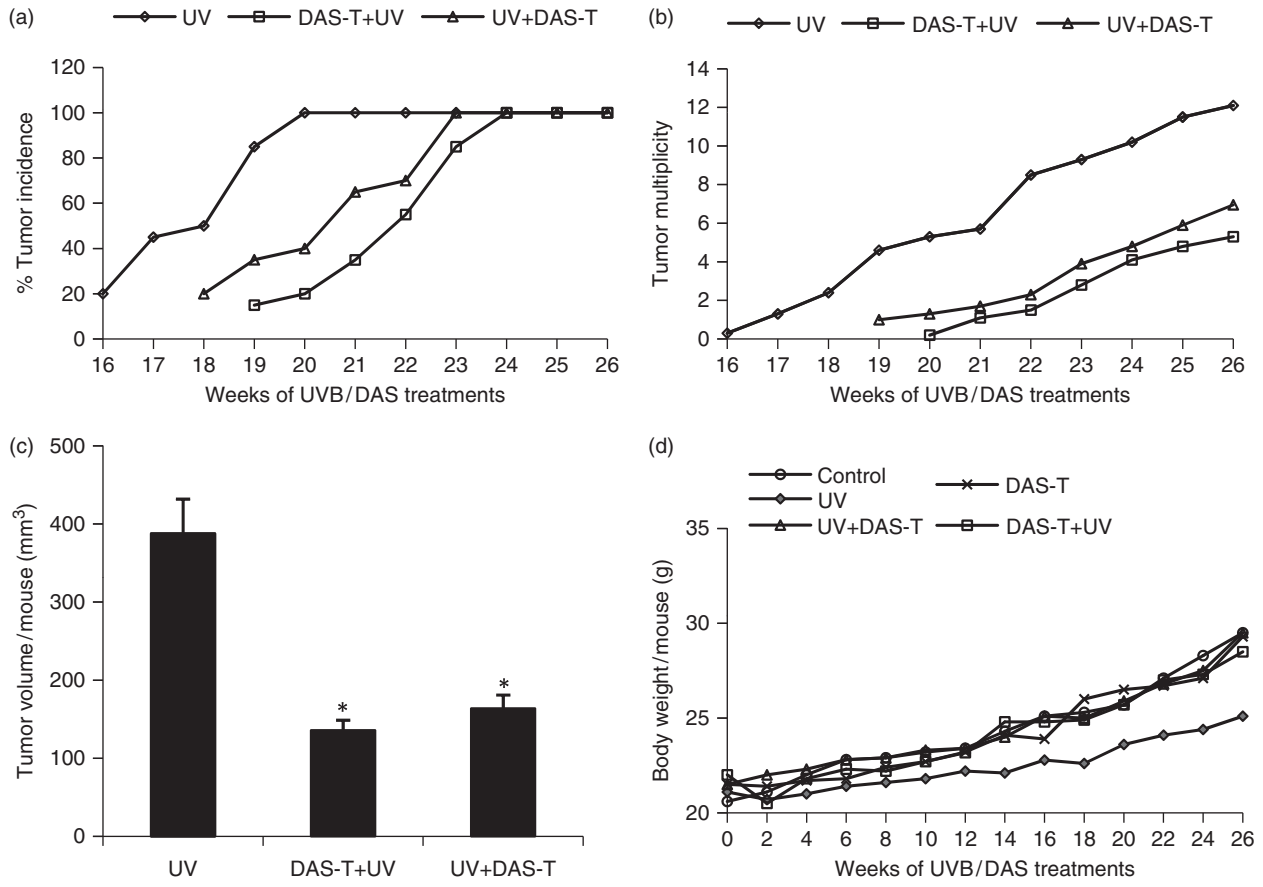

Fig. 1. Effect of diallyl sulfide (DAS) on ultraviolet B (UVB)-induced skin photocarcinogenesis in SKH-1 hairless mouse. The results were obtained from the long-term regimen shown in Table 1. Experiment was terminated at 26 weeks after UVB exposure. Percentage of tumor incidence (a), tumor multiplicity per mouse (b), tumor volume per mouse (c), and body weight per mouse (d) were recorded and analyzed. The data shown in (c) are mean ± SE (bars). In each case, the data shown are from 20 mice in each group. No tumors were observed in the control and the topically treated DAS-alone groups; therefore, these data are not shown. *$P < 0.005$ versus the group.

(data not shown). None of the DAS treatments caused any significant decrease in diet consumption or body weight change (Fig. 1d), indicating no observable toxicity in SKH-1 mouse skin.

DAS inhibits UVB-induced apoptosis and apoptotic sunburn cell formation

Compared with unexposed control mice (Fig. 2a), the topical application of DAS (DAS-T) (Fig. 2c) did not induce apoptotic cells *per se*. UVB exposure significantly induced TUNEL-positive apoptotic cells (Fig. 2b). Both DAS-T+UV and UV+DAS-T (result not shown) revealed a significant suppression in UVB-induced apoptosis. Consistent with the above results, quantitative analysis (Fig. 2e) revealed that UVB irradiation resulted in $28.8 \pm 2.61\%$ TUNEL-positive apoptotic cells, while a low level of these apoptotic cells was observed in the unirradiated control or in the DAS-T group ($2.7 \pm 0.49\%$ and $2.5 \pm 0.35\%$, respectively). Both DAS-T+UV and UV+DAS-T groups decreased the TUNEL-positive apoptotic cells to $11.4 \pm 1.97\%$ and $15.2 \pm 2.12\%$, respectively, accounting for 60% and 47% inhibition ($P < 0.006$).

Characteristic dyskeratotic sunburn cells with pyknotic nuclei were detected by histomorphologic analysis using H&E staining. Compared with unexposed control mice, UVB exposure alone significantly increased UVB-induced H&E-positive apoptotic sunburn cells from $0.94 \pm 0.16\%$ (control) or $0.92 \pm 0.11\%$ (DAS-T) to $11.5 \pm 1.63\%$ (Fig. 2f). DAS-T+UV and UV+DAS-T resulted in $3.6 \pm 0.42\%$ and $4.7 \pm 0.64\%$ apoptotic sunburn cells, respectively, accounting for 68% and 59% inhibition ($P < 0.005$).

Protective effects of DAS on UV-induced thymine dimers

Thymine dimers are considered as an early important biomarker for UVB-induced DNA damage (21). Compared with sham-irradiated controls (Fig. 3a), 1 h after a single exposure of mice to UVB, the formation of thymine dimer-positive cells was strongly induced (Fig. 3b). However, in the DAS-T+UV group (Fig. 3c) and in the UV+DAS-T group (data not shown), a similar level of reduction in the thymine dimer-positive population was found. UVB alone resulted in $91 \pm 4.9\%$ thymine dimer-positive cells in the epidermis, while negligible levels of these cells were observed

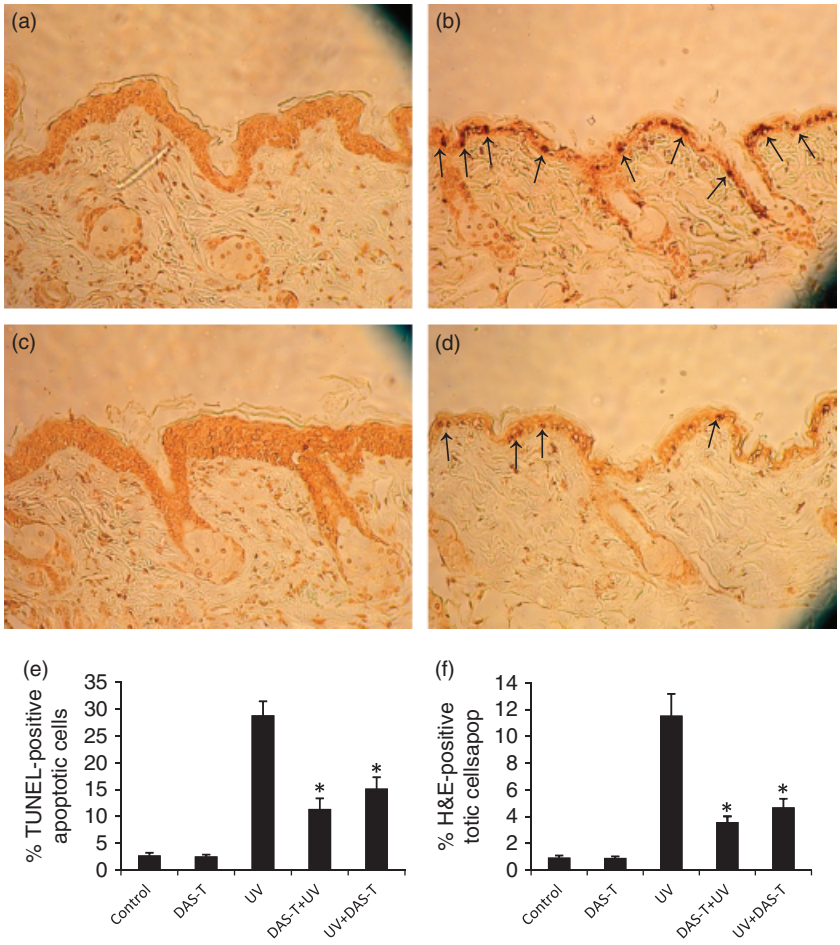

Fig. 2. Inhibition of ultraviolet B (UVB)-induced apoptosis by diallyl sulfide (DAS). The apoptotic cells were detected using the TUNEL assay and H&E staining. (a) Control; (b) UV; (c) DAS-T+UV; (d) UV+DAS-T. Arrows show apoptotic cells with brown staining. The quantitative results of TUNEL-positive cells (e) and H&E-positive cells (f) were statistically analyzed. Data were calculated as mean ± SE of 25 fields/5 mice/group. *$P < 0.006$ (TUNEL), *$P < 0.005$ (H&E).

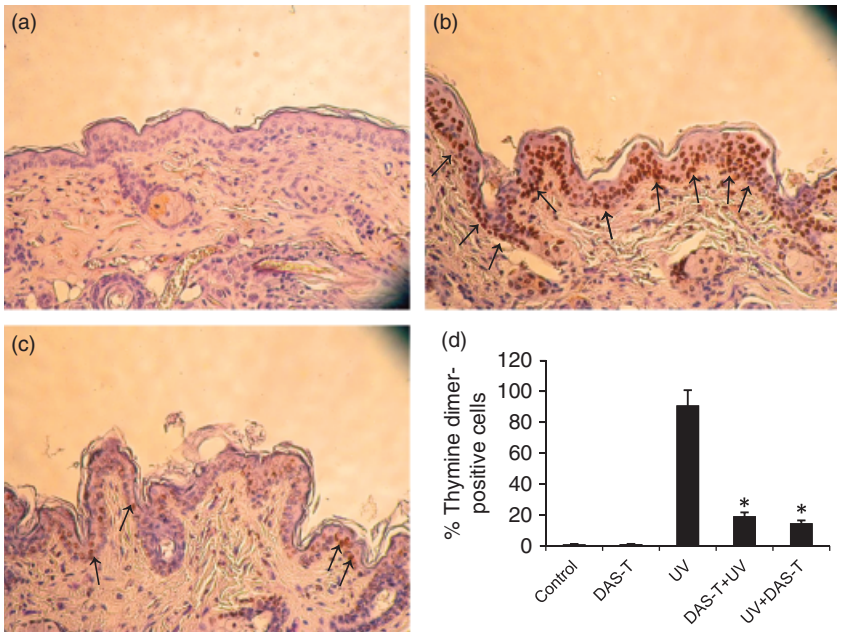

Fig. 3. Inhibition of ultraviolet B (UVB)-induced thymine dimer formation by diallyl sulfide (DAS). (a) Control; (b) UV; and (c) (DAS-T+UV). Arrows show thymine dimer-positive cells with brown staining. The results of UV+DAS-T treatment were similar to that of DAS-T+UV (data not shown). Thus, the data of UV+DAS-T in the subsequent figures are not shown but are presented in the quantitative data. (d) Quantitative results of thymine dimer-positive cell populations. $^{*}P < 0.002$.

in unirradiated controls ($1.1 \pm 0.14\%$) or topical ($1.2 \pm 0.13\%$) DAS-T alone (Fig. 3d). In contrast, DAS-T+UV and UV+DAS-T resulted in a similar level of reduction in thymine dimer-positive cells (19.3 ± 2.5 vs 14.8 ± 1.8), accounting for 79% and 84% inhibition ($P < 0.002$).

Effects of DAS on UVB-induced upregulation of the p53–p21/Cip1 cascade

Compared with unexposed and untreated controls showing almost no reactivity for p53 immunostaining (Fig. 4a, d), UVB exposure alone remarkably increased the p53-positive cells (Fig. 4b), which were seen primarily in the basal layer, but some were also observed in the suprabasal layer of the epidermis near the basal layer. Further increase in the numbers of p53-positive cells was observed in the DAS-T+UV group (Fig. 4c). Quantitative analysis (Fig. 4d) revealed that UVB irradiation resulted in $33.5 \pm 3.5\%$ p53-positive cells in the epidermis, while low levels of these cells were observed in the unirradiated control (1.85 ± 0.21), or DAS-T ($1.95 \pm 0.21\%$). Moreover, both DAS-T+UV and UV+DAS-T resulted in $61 \pm 7.1\%$ and $54.8 \pm 6.0\%$, p53-positive cells, accounting for 79% and 62% enhancement ($P < 0.02$).

Similarly, compared with the unexposed control (Fig. 5a), UVB exposure alone significantly increased the p21/Cip-1-positive cells (Fig. 5b), which were further enhanced in the DAS-T+UV group (Fig. 5c). Quantitative analysis revealed that UVB irradiation resulted in $13.02 \pm 0.71\%$ p21/Cip1-positive cells in the epidermis (Fig. 5d), while a low level of these cells was observed in the unirradiated control ($1.25 \pm 0.07\%$) or DAS-T ($1.34 \pm 0.08\%$). In contrast, the p21/Cip1-positive cells were significantly increased in the DAS-T+UV and UV+DAS-T groups, $23.2 \pm 1.2\%$ and $24.5 \pm 1.4\%$, respectively, accounting for 78% and 88% enhancement ($P < 0.003$).

DAS suppresses UV-induced cell proliferation

PCNA-positive cells were low in the unexposed control (Fig. 6a), but were markedly increased upon UVB exposure (Fig. 6b). However, these cells were significantly decreased in the DAS-T+UV group (Fig. 6c). Quantitative analysis (Fig. 6d) showed $1.9 \pm 0.14\%$ and $2.17 \pm 0.24\%$ of PCNA-positive cells in the control and DAS-T groups. In contrast, these cells were markedly increased to $28.1 \pm 1.6\%$ by UVB irradiation, but were decreased in the DAS-T+UV (13.6 ± 0.6) and UV+DAS-T ($15.7 \pm 1.0\%$) groups, accounting for 51% and 44% inhibition ($P < 0.002$).

DAS inhibits UVB-induced activation of NF-κB, COX-2, NO, and PEG2 levels

We next examined the effects of UVB exposure without or with DAS treatments on the activities of cellular factors associated with skin tumorigenesis. Figure 7a shows that UVB exposure alone significantly increased the activity of NF-κB from 0.15 ± 0.01 in control and 0.16 ± 0.01 in DAS-T to 0.58 ± 0.04. However, NF-κB activity was decreased to 0.25 ± 0.03 and 0.31 ± 0.04 in DAS-T+UV and UV+DAS-T, respectively ($P < 0.004$).

Figure 7b shows an increased COX-2 activity (0.93 ± 0.06) in response to UVB irradiation, but was significantly decreased by DAS-T+UV (0.61 ± 0.04) and UV+DAS-T (0.56 ± 0.03).

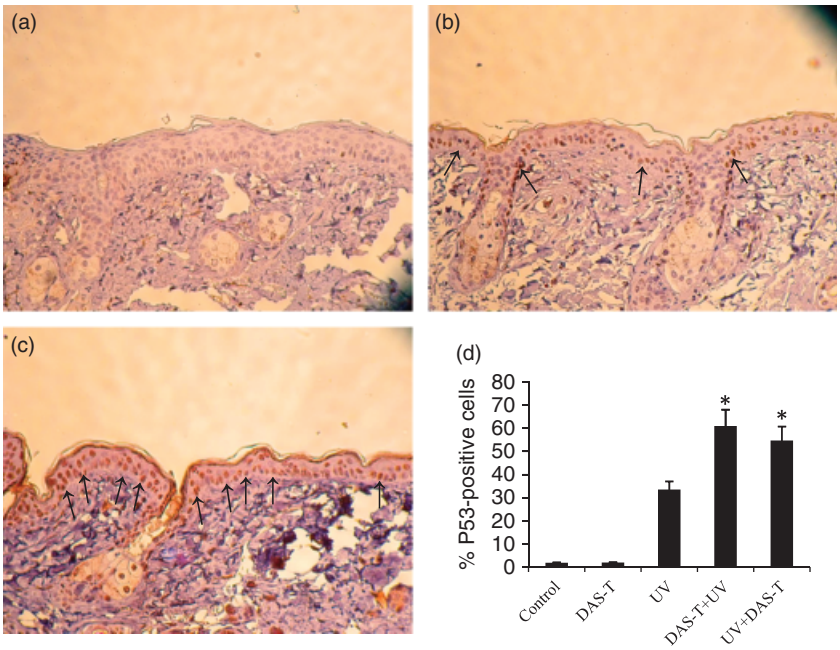

Fig. 4. Diallyl sulfide (DAS) enhances ultraviolet B (UVB)-induced p53 expression. (a) Control; (b) UV; (c) DAS-T+UV. Arrows show p53-positive cells with brown staining. (d) Quantitative results of p53-positive cell populations under five different experimental conditions. $^{*}P < 0.02$.

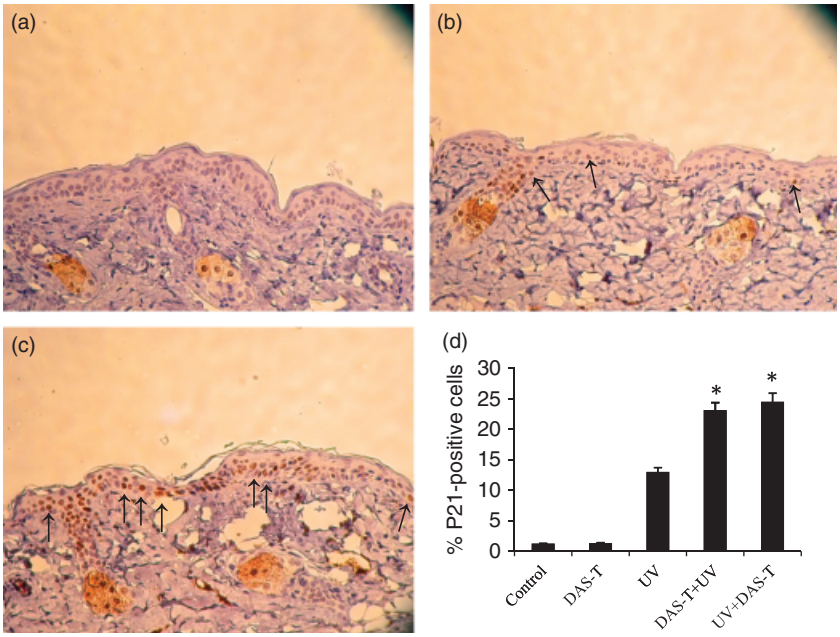

Fig. 5. Diallyl sulfide (DAS) enhances ultraviolet B (UVB)-induced p21/Cip1 expression. (a) Control; (b) UV; (c) DAS-T+UV. (d) Quantitative results of p21-positive cell populations under five different experimental conditions. $^{*}P < 0.003$.

Similar background levels of COX-2 activity were observed in the unirradiated control (0.35 ± 0.02) or DAS-T (0.33 ± 0.02); thus, DAS treatment resulted in 34% and 39% inhibition of COX-2 activity, respectively.

Similarly, UVB exposure alone resulted in an NO activity of $470 \pm 28.3\%$ relative to that in the unirradiated control (102 ± 12), accounting for an approximately 3.7-fold increase (Fig. 7c). DAS-T did not affect the NO *per se*. However, both DAS-T+UV and UV+DAS-T resulted in a significant reduction of NO activity.

Figure 7d showed that PGE2 activity (376 ± 22.7) markedly increased above the control level in response to UVB irradiation, but was significantly decreased in DAS-T+UV (217.5 ± 17.7) and UV+DAS-T (246 ± 19.8), resulting in net reductions of 42% and 35% of PGE2 activity. Topical DAS treatment by itself did not affect the activity of PEG2 *per se*.

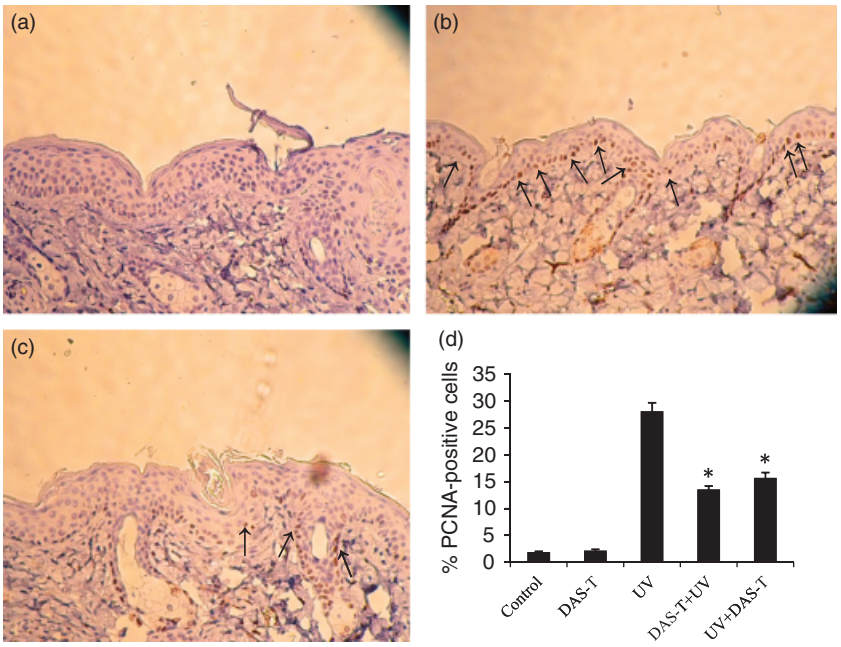

Fig. 6. Inhibition of ultraviolet B (UVB)-induced proliferative cell nuclear antigen (PCNA)-positive cells by diallyl sulfide (DAS). (a) Control; (b) UV; (c) DAS-T+UV. (d) Quantitative results of PCNA-positive cell populations under five different experimental conditions. $^{*}P < 0.002$.

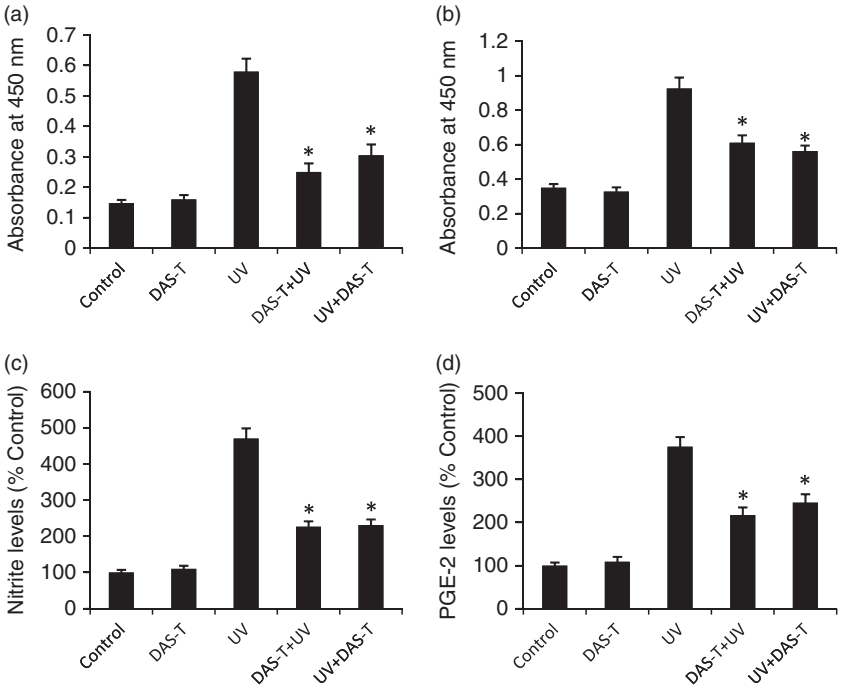

Fig. 7. Inhibition of ultraviolet B (UVB)-induced activation of nuclear factor-κB (NF-κB), cyclooxygenase-2 (COX-2), nitric oxide (NO), and prostaglandin E2 (PGE2) expressions by diallyl sulfide (DAS). Skin lysates were analyzed for NF-κB, COX-2, NO, and PGE2 activities. (a) NF-κB; (b) COX-2; (c) NO; and (d) PGE2. Activities were calculated as mean ± SE (n = 5). $^{*}P < 0.004$ (NF-κB), $^{*}P < 0.007$ (COX-2), $^{*}P < 0.002$ (NO), $^{*}P < 0.006$ (PGE2).

Discussion

The major findings in the present study are that topical application of DAS caused a delay and a reduction in UVB-induced tumor appearance, multiplicity, and size in hairless mice without any toxicity. Based on the results showing an inhibition of tumor growth by DAS in UVB-induced tumorigenesis, we then investigated the early molecular events associated with the inhibitory effects of DAS by using immunohistochemical and morphological methods, which allowed multiple measures on serial sections from the same skin samples.

The results indicated that the administration of DAS to SKH-1 mice inhibits UVB-induced carcinogenesis at several mechanistically different levels. Previous reports showed that UV irradiation exerts its cytotoxic and carcinogenetic effects mainly through the direct formation of cyclobutane pyrimidine dimmers (22, 23). Thymine dimers are considered as an early and important biomarker for UVB-induced DNA damage. In the present study, we observed that the application of DAS both before and immediately after UVB irradiation inhibited UVB-induced formation of thymine dimers and sunburn lesions to a similar extent. These results indicated that DAS can inhibit UVB-induced carcinogenesis by mechanisms independent of its possible 'sunscreening' effects.

A previous report indicated that in response to DNA damage by UV irradiation, p53 and p21/Cip1 are up-regulated for cell cycle arrest to facilitate DNA repair (24). Peak increases in the number of p53-positive epidermal cells occurred at 8–12 h after exposure to UVB (24). UV-induced increase in p53 protein accumulation is known to be accompanied by the enhanced synthesis of p21/Cip1 protein, which plays a crucial role in the adaptive responses after UV exposure of the skin by inhibiting cell proliferation (25). The antiproliferative effect of DAS against UVB-induced tumor growth might also involve cell cycle regulatory mechanisms. Our results showed that DAS increased the protein expression of the Cdk inhibitor, p21/Cip1, which is well known to interact with and inhibit the kinase activity of the Cdk–cyclin complex. In our study, DAS treatment resulted in a further increase in UV-induced p53 accumulation with a concomitant increase in the p21/Cip1 protein levels, which is in agreement with the inhibition of UV-induced cell proliferation and apoptosis by DAS, suggesting their possible role in cell growth inhibition rather than apoptosis induction. Thus, UVB-induced DNA damage, cell proliferation, and apoptotic sunburn cell formation are prevented by DAS possibly via further induction in the p53–p21/Cip1 cascade.

Persistent inflammation causes hyperproliferation in the epidermis and an enhanced proliferation rate is the hallmark of tumor cells. UV-induced increase in cell proliferation is an early necessary event associated with UV-caused carcinogenesis that helps the initiated cells to proceed further into the cell cycle (26); this response, however, could be prevented by arresting the cells at the G1 or the S phase of the cell cycle. We observed that UVB-induced PCNA-positive cells were strongly inhibited by DAS treatment. These results suggest that inhibiting cell proliferation could be one of the mechanisms by which DAS protects damaged cells by providing additional time for repair and preventing their entry into the apoptotic pathway in case the damage is severe. This suggestion is in agreement with the observation that DAS treatment further up-regulates p21/Cip1 levels, which is known to inhibit cell proliferation by direct binding with PCNA (27).

Previous reports indicated that transcription factor NF-κB plays a central role in the early events of UV-induced skin damage such as general inflammatory as well as immune responses. Several chemopreventive phytochemicals have been shown to inhibit COX-2 and iNOS expression by blocking improper NF-κB activation (28–30). In addition, it has been suggested that UV-induced prostaglandin (PGE) synthesis may also be a significant contributing factor in UV-induced skin tumorigenesis (31). iNOS produces biological NO that plays a pivotal role in UV-induced inflammation and is implicated in the pathogenesis of various inflammatory diseases, including sunburn and pigmentation, as well as in different stages of tumorigenesis (32). Our study showed that a single exposure of UVB strongly induced NO expression in mouse skin, which is clinically relevant, as in humans, photosensitivity is shown to be positively associated with the level of iNOS expression (33). Thus, down-regulation of UVB-induced nitrite expression by DAS was possibly associated with its photoprotective effects.

COX-2 is a key enzyme required for PGEs syntheses that mediate inflammatory responses. Recent studies indicate a link between iNOS and COX-2 expression (34). Consistent with this report, our study showed increased COX-2 and PGE2 levels in UVB-exposed mouse skin and DAS treatments substantially lowered COX-2 and PGE2 protein levels. Together, these findings suggest that a single exposure of UVB induces iNOS and COX-2 to mediate inflammatory and related processes *in vivo* and that topical DAS treatment could effectively suppress them.

The transcription factor NF-κB is associated with diverse activities linked to growth-promoting potential and antiapoptotic responses of cells to a broad spectrum of stimuli that may result in the malignant transformation of cells acquiring drug resistance and metastatic potential. The activation of NF-κB by UVB shown in this study suggests that it could be a clinically relevant target to protect from photodamage and photocarcinogenesis. The inhibitory effect of DAS reported in the present study supported this notion.

In summary, our results in this study suggest that DAS not only reduces DNA damage with the activation of the p53–p21/Cip1 cascade but also inhibits NF-κB and COX-2 with suppression of NO and PGE2, resulting in decreased cell proliferation and apoptosis in UV-irradiated SKH-1 hairless mouse epidermis. The present study provides fundamental information on the effects of DAS on mechanistically important early biomarkers for UVB-caused effects *in vivo*, suggesting a model for the evaluation of potential protective pharmacological modulators against UVB-induced damages. More mechanistic studies are needed in future to further clarify the effect of DAS on UV-induced damage, and their biological significance in both the overall efficacy and the safety of DAS against UV-induced skin damage. Our results warrant the development of DAS as a safe and effective chemopreventive agent against UV-induced photoaging and photocarcinogenesis.

Acknowledgments

This work was supported in part by grants from the National Science Council (NSC) of Taiwan (97-2320-B-040-033-MY3), China Medical University Beigang Hospital, Taiwan.

References

1. Armstrong BK, Kricker A. The epidemiology of UV induced skin cancer. *J Photochem Photobiol B* 2001; **63**: 8–18.

2. Heck DE, Vetrano AM, Mariano TM, Laskin JD. UVB light stimulates production of reactive oxygen species: unexpected role for catalase. *J Biol Chem* 2003; **278**: 22432–22436.
3. Ananthaswamy HN. Ultraviolet light as a carcinogen. In: Bowden GT, Fischer S.M, eds. *Comprehensive toxicology*. NY: Elsevier, 1997; 255–279.
4. Abdullah TH, Kandil O, Elkadi A, Carter J. Garlic revisited: therapeutic for the major diseases of our times? *J Natl Med Assoc* 1988; **80**: 439–445.
5. Ross IA. *Medicinal plants of the world*. Humana Press, 2003.
6. Smyth AR, Cifelli PM, Ortori CA, *et al*. Garlic as an inhibitor of *Pseudomonas aeruginosa* quorum sensing in cystic fibrosis – a pilot randomized controlled trial. *Pediatr Pulmonol* 2010; **45**: 356–362.
7. Yang CS, Chhabra SK, Hong JY, Smith TJ. Mechanisms of inhibition of chemical toxicity and carcinogenesis by diallyl sulfide (DAS) and related compounds from garlic. *J Nutr* 2001; **131**: 1041S–1045S.
8. Ban JO, Oh JH, Kim TM, *et al*. Anti-inflammatory and arthritic effects of thiacremonone, a novel sulfur compound isolated from garlic via inhibition of NF-kappaB. *Arthritis Res Ther* 2009; **11**: R145.
9. Zhang Y, Yao HP, Huang FF, *et al*. Allicin, a major component of garlic, inhibits apoptosis in vital organs in rats with trauma/hemorrhagic shock. *Crit Care Med* 2008; **36**: 3226–3232.
10. Chang HP, Chen YH. Differential effects of organosulfur compounds from garlic oil on nitric oxide and prostaglandin E2 in stimulated macrophages. *Nutrition* 2005; **21**: 530–536.
11. Mordan LJ, Burnett TS, Zhang LX, Tom J, Cooney RV. Inhibitors of endogenous nitrogen oxide formation block the promotion of neoplastic transformation in C3 H 10T1/2 fibroblasts. *Carcinogenesis* 1993; **14**: 1555–1559.
12. Gallo O, Masini E, Morbidelli L, *et al*. Role of nitric oxide in angiogenesis and tumor progression in head and neck cancer. *J Natl Cancer Inst* 1998; **90**: 587–596.
13. Ban JO, Yuk DY, Woo KS, *et al*. Inhibition of cell growth and induction of apoptosis via inactivation of NF-kappaB by a sulfurcompound isolated from garlic in human colon cancer cells. *J Pharmacol Sci* 2007; **104**: 374–383.
14. Winkelmann RK, Baldes EJ, Zollman PE. Squamous cell tumors induced in hairless mice with ultraviolet light. *J Invest Dermatol* 1960; **34**: 131–138.
15. Epstein JH, Epstein WL. A study of tumor types produced by ultraviolet light in hairless and hairy mice. *J Invest Dermatol* 1963; **41**: 463–473.
16. Epstein JH. Comparison of the carcinogenic and cocarcinogenic effects of ultraviolet light on hairless mice. *J Natl Cancer Inst* 1965; **34**: 741–745.
17. Winkelmann RK, Zollman PE, Baldes EJ. Squamous cell carcinoma produced by ultraviolet light in hairless mice. *J Invest Dermatol* 1963; **40**: 217–224.
18. Black HS, Chiang J, Gerguis J, Lenger W, Thornby JI. Biochemical parameters of epidermal aging in the hairless mouse and the relationship to UV-carcinogenesis. *J Photochem Photobiol B* 1994; **23**: 111–118.
19. Hersh L, Fukuyama K, Inoue N, Epstein JH. Immunofluorescent studies of epidermal protein during UV induced carcinogenesis. *Virchows Arch B Cell Pathol* 1977; **24**: 157–164.
20. Cherng JM, Lin HJ, Hung MS, Lin YR, Chan MH, Lin JC. Inhibition of nuclear factor kappaB is associated with neuroprotective effects of glycyrrhizic acid on glutamate-induced excitotoxicity in primary neurons. *Eur J Pharmacol* 2006; **547**: 10–21.
21. Lu YP, Lou YR, Yen P, Mitchell D, Huang MT, Conney AH. Time course for early adaptive responses to ultraviolet B light in the epidermis of SKH-1 mice. *Cancer Res* 1999; **59**: 4591–4602.
22. Hart RW, Setlow RB, Woodhead AD. Evidence that pyrimidine dimers in DNA can give rise to tumors. *Proc Natl Acad Sci USA* 1977; **74**: 5574–5578.
23. Dhanalakshmi S, Mallikarjuna GU, Singh RP, Agarwal R. Silibinin prevents ultraviolet radiation-caused skin damages in SKH-1 hairless mice via a decrease in thymine dimer positive cells and an up-regulation of p53-p21/Cip1 in epidermis. *Carcinogenesis* 2004; **25**: 1459–1465.
24. Ponten F, Berne B, Ren ZP, Nister M, Ponten J. Ultraviolet light induces expression of p53 and p21 in human skin: effect of sunscreen and constitutive p21 expression in skin appendages. *J Invest Dermatol* 1995; **105**: 402–406.
25. Huang LC, Clarkin KC, Wahl GM. Sensitivity and selectivity of the DNA damage sensor responsible for activating p53-dependent G1 arrest. *Proc Natl Acad Sci USA* 1996; **93**: 4827–4832.
26. Gu M, Singh RP, Dhanalakshmi S, Mohan S, Agarwal R. Differential effect of silibinin on E2F transcription factors and associated biological events in chronically UVB-exposed skin versus tumors in SKH-1 hairless mice. *Mol Cancer Ther* 2006; **5**: 2121–2129.
27. Ducoux M, Urbach S, Baldacci G, *et al*. Mediation of proliferating cell nuclear antigen (PCNA)-dependent DNA replication through a conserved p21(Cip1)-like PCNA-binding motif present in the third subunit of human DNA polymerase delta. *J Biol Chem* 2001; **276**: 49258–49266.
28. Surh YJ, Chun KS, Cha HH, *et al*. Molecular mechanisms underlying chemopreventive activities of anti-inflammatory phytochemicals: down-regulation of COX-2 and iNOS through suppression of NF-kappa B activation. *Mutat Res* 2001; **480–481**: 243–268.
29. Singh S, Aggarwal BB. Activation of transcription factor NF-kappa B is suppressed by curcumin (diferuloylmethane). *J Biol Chem* 1995; **270**: 24995–25000.
30. Lyss G, Schmidt TJ, Merfort I, Pahl HL. Helenalin, an anti-inflammatory sesquiterpene lactone from Arnica, selectively inhibits transcription factor NF-kappaB. *Biol Chem* 1997; **378**: 951–961.
31. Grewe M, Trefzer U, Ballhorn A, Gyufko K, Henninger H, Krutmann J. Analysis of the mechanism of ultraviolet (UV) B radiation-induced prostaglandin E2 synthesis by human epidermoid carcinoma cells. *J Invest Dermatol* 1993; **101**: 528–531.
32. Chiang YM, Lo CP, Chen YP, *et al*. Ethyl caffeate suppresses NF-kappaB activation and its downstream inflammatory mediators, iNOS, COX-2, and PGE2 in vitro or in mouse skin. *Br J Pharmacol* 2005; **146**: 352–363.
33. Tsukazaki N, Watanabe M, Shimizu K, Hamasaki Y, Katayama I. Photoprovocation test and immunohistochemical analysis of inducible nitric oxide synthase expression in patients with Sjogren's syndrome associated with photosensitivity. *Br J Dermatol* 2002; **147**: 1102–1108.
34. Yoshida E, Watanabe T, Takata J, Yamazaki A, Karube Y, Kobayashi S. Topical application of a novel, hydrophilic gamma-tocopherol derivative reduces photo-inflammation in mice skin. *J Invest Dermatol* 2006; **126**: 1633–1640.